JTTEE5 7:43-46

Thermal Conductivity of a Zirconia Thermal Barrier Coating

A.J. Slifka, B.J. Filla, J.M. Phelps, G. Bancke, and C.C. Berndt

(Submitted 17 April 1997; in revised form 9 October 1997)

The conductivity of a thermal-barrier coating composed of atmospheric plasma sprayed 8 mass percent yttria partially stabilized zirconia has been measured. This coating was sprayed on a substrate of 410 stainless steel. An absolute, steady-state measurement method was used to measure thermal conductivity from 400 to 800 K. The thermal conductivity of the coating is 0.62 W/(m·K). This measurement has shown to be temperature independent.

Keywords thermal barrier coating, thermal conductivity, thermal resistance, zirconia

1. Introduction

The thermal conductivity of a ceramic-thermal-barrier coating was directly measured. It is often used in gas turbine engine applications (Ref 1). Although a variety of deposition techniques are used, plasma spray is a common technique for applying coatings on metallic substrates. The coating insulates the underlying superalloy material, thus reducing its operating temperature and extending the life of the engine. Coatings currently used in gas turbine engines are not prime-reliant, since even if the coatings are removed, the engine will still operate within the thermal limits of the superalloy materials. A material is prime reliant if the integrity of the material is necessary for the operation of the engine. A prime reliant coating is used to extend the operating temperature of the engine, hence increasing its efficiency (Ref 2). The primary factor precluding this is spallation of the coating (Ref 3). A second factor is the lack of accurate and reliable measurements of the thermal conductivity of the coating.

The most common industrial technique used to measure thermal conductivity is the laser-flash method. The laser-flash technique is fast and relatively simple to perform, but measures thermal diffusivity. Calculation of thermal conductivity from thermal diffusivity requires values for density and specific heat at the exact temperature the diffusivity is measured.

Due to the inhomogeneous and anisotropic structures possible in plasma-sprayed materials (Ref 4), values of bulk density and specific heat, often given for only a fixed temperature, may not yield values for thermal conductivity with suitable accuracy. However, fundamental measurement of thermal conductivity would eliminate some of the uncertainty in the calculated thermal conductivity values derived from measurements of thermal diffusivity. Correlating direct, steady-state measurements of thermal conductivity and transient measurements of thermal diffusivity is the first step in developing a high-temperature standard-reference material (SRM) for the measurement of thermal conductivity of ceramic coatings.

A.J. Slifka, **B.J. Filla**, and **J.M. Phelps,** Materials Reliability Division, National Institute of Standards and Technology, Boulder, CO 80303, USA; **G. Bancke** and **C.C. Berndt,** Thermal Spray Laboratory, Materials Science and Engineering, State University of New York at Stony Brook, Stony Brook, NY 11794, USA.

2. Measurement Method

The thermal conductivity of an 8 mass percent yttria partially stabilized zirconia (8YSZ) atmospheric plasma-sprayed thermal barrier coating was measured using an absolute, steady-state measurement technique. A one-sided guarded hot plate (GHP) based, in principle, on the ASTM C 177-85 standard test method (Ref 5) was used. Details of the design of the apparatus are found elsewhere (Ref 6 & 7). Figure 1 shows a schematic of the salient features of the measurement system. The back-guarded, one-sided nature of the apparatus reduces heat loss and requires only one specimen rather than two, as specified in ASTM C 177-85. The principle of operation is to create one-dimensional axial heat flow through the sample in order to use the Fourier equation of heat conduction:

$$q = -kA \frac{dT}{dx}$$

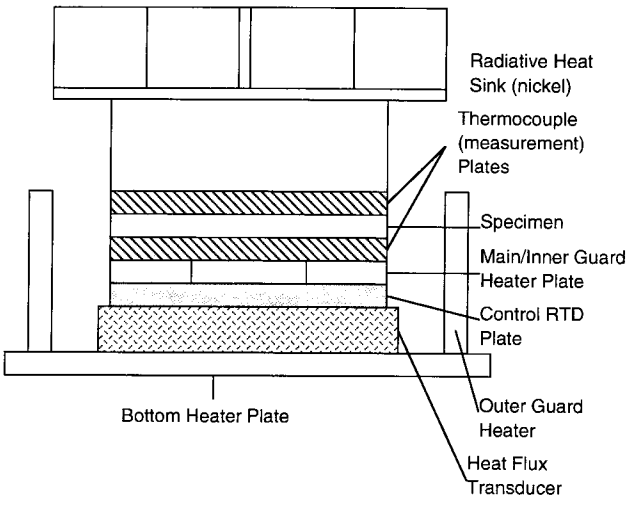

Fig. 1 Schematic of the measurement stack of the guarded hot plate

where q is the steady-state flow, k is thermal conductivity, A is the cross-sectional area of the sample, and –dT/dx is the temperature gradient (Ref 8). A central stack of heater and sensor plates surrounded by a cylindrical outer guard was used to generate one-dimensional axial heat flow upward through the specimen to the heat sink. A uniform power density is applied to the main/inner guard heater plate to obtain a specified temperature at the control-RTD (resistance temperature detector). The main/inner guard plate has separate heater elements: one central main heater, and a second, annular inner-guard heater surrounding the main heater. The power input to the main heater is measured and used in the Fourier heat equation to calculate thermal conductivity.

The principle of a GHP is to direct all the heat generated by the main heater to flow axially through the specimen. This is currently accomplished by the inner and outer guards and bottom heater plate, all controlled to operate at the same temperature as the main heater. Heat flux in the main heater does not flow radially because the controlled inner guard ensures that there is no radial temperature gradient within the main heater. Controlling the bottom heater to the same temperature as the main heater permits no heat to descend from the main heater to the measurement stack. The outer guard is also controlled to the same temperature as the main/inner guard plate so that no heat is lost radially from the inner guard. These heaters permit heat to flow only upward through the specimen and thermocouple plates to the heat sink, where it is radiated away to the cooler furnace. In this way, known heat input to the main heater, measurement of dT/dx across the specimen using the thermocouple plates, and knowledge of the cross-sectional area of heat flow yield the raw data needed to calculate thermal conductivity.

The raw data, however, not only include the thermal resistance of the specimen, but also the finite thermal resistance between the specimen and the thermocouple plates. The thermal resistance between the thermocouple plates and specimen depends on the surface finish of the specimen and the oxidative behavior of the specimen.

Since the present specimens are ceramic coatings that were atmospheric plasma sprayed on metallic substrates, there are five thermal resistances to consider: the thermal resistances of the coating and substrate, the interfacial resistance between the coating and substrate, the interfacial resistances between the coating or substrate, and the two thermocouple plates. The test environment is 50 kPa helium to obtain good thermal coupling between the specimen and measurement plates. Initially, two different thicknesses of uncoated substrate material blanks were measured to determine the thermal resistance between the substrate material and thermocouple plate, and the thermal conductivity of the substrate material. The substrate and interfacial resistance were then subtracted from the total resistance of the coated specimens. Using the net resistances for each of two coated specimens of different thickness, the interfacial resistance between the coating and thermocouple plate and the coating thermal conductivity was determined.

The coating measured here had a NiCrAlY bond coat between the substrate and 8YSZ coating. Since thermal barrier coatings using NiCrAlY bond coats typically survive for hundreds of thermal cycles (Ref 9), the mechanical contact between bond coat and substrate and bond coat and coating can be assumed to be adequate to neglect the thermal resistance at the coating/substrate interface. In these measurements, the thermal resistance of the coating includes this small resistance.

3. Results

The atmospheric plasma-sprayed 8YSZ specimens were produced at the State University of New York at Stony Brook. All coatings were sprayed on 69.85 mm diameter substrates of 410 stainless steel with a 0.1 mm thick NiCrAlY bond coat. The 8YSZ coatings were atmospheric plasma sprayed using a Sulzer-Metco (Westbury, NY) designation SP10655 powder*

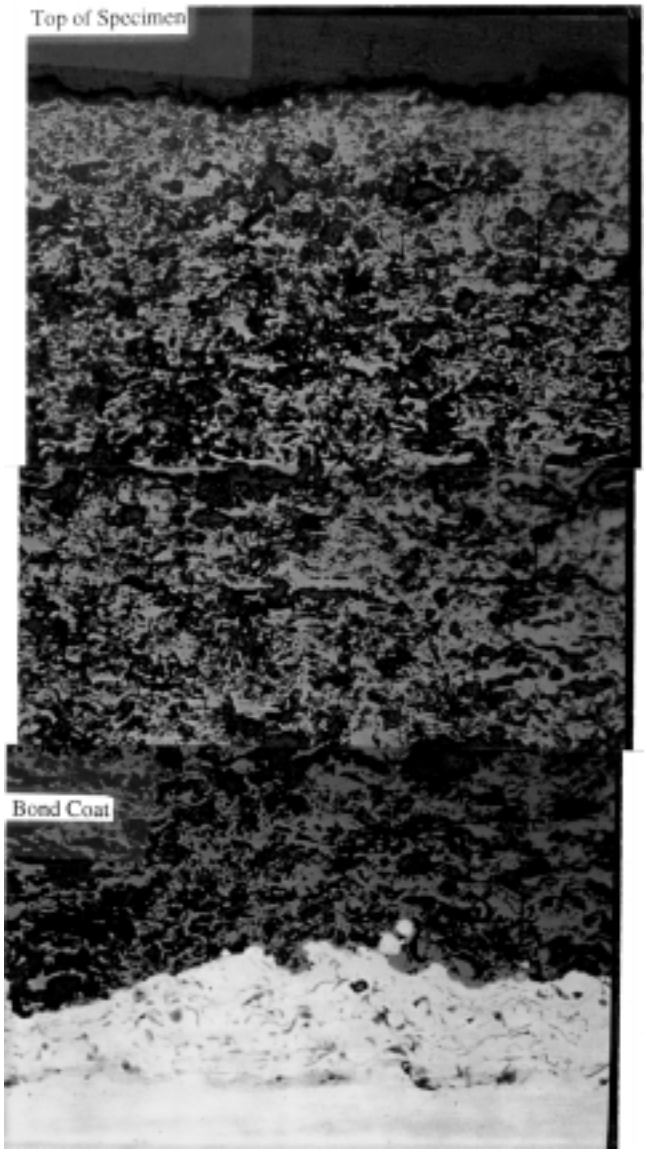

Fig. 2 Composite optical micrograph showing the typical splat structure of the atmospheric plasma-sprayed 8YSZ coating. 20×. (Art has been reduced to 74% of its original size for printing.)

*Identification given for scientific accuracy in the description of the process. No endorsement of this product by NIST is intended or implied.

for 200, 400, and 680 cycles, resulting, respectively, in 1.0, 2.0, and 3.0 mm thick coatings. One cycle corresponds to a complete (down and up) traverse of the torch across the sample, with the torch traveling at 20 mm/s at a spray distance of 130 mm. The substrate is rotated at 160 rev/min during the spray operation.

Figure 2 shows the typical splat-type microstructure of the coatings. As mentioned, the thermal resistances between the substrate and bond coat and between the bond coat and coating are negligible. In addition, the bond coat is treated as additional substrate because the NiCrAlY bond coat has a thermal conductivity close to that of 410 stainless steel (Ref 10). The coating porosity was estimated as 16.5% by measuring the volume and mass of the sample. X-ray diffraction analysis shows the presence of all three phases of zirconia, but predominantly tetragonal, and is consistent with the structure of a plasma-sprayed coating using a commercial powder (Ref 11).

Three stainless steel substrate blanks of 1.93, 3.94, and 8.00 mm thicknesses were first measured. The thermal conductivity and interfacial resistance between the measurement plates and 410 stainless steel were measured from 400 to 800 K. Figure 3 shows thermal conductivity data for 410 stainless steel measured in the GHP. The values obtained are consistent with literature values for series 400 stainless steels (Ref 12). Figure 4 shows interfacial resistance data determined from the 410 stainless steel test runs. These data are reported in units that are not dependent on the size of the device used for measurement. The tests start at 475 K and increase in steps of 100 K up to the maximum temperature; they then drop down to 375 K and step at in-

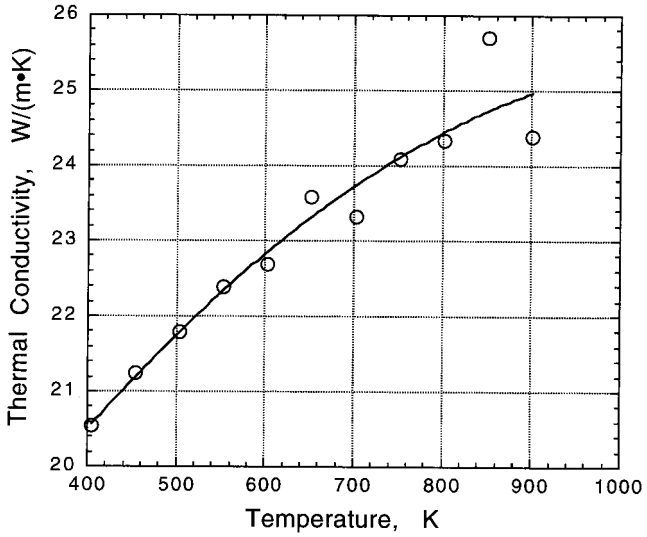

Fig. 3 Thermal conductivity of 410 stainless steel as measured in the guarded hot plate

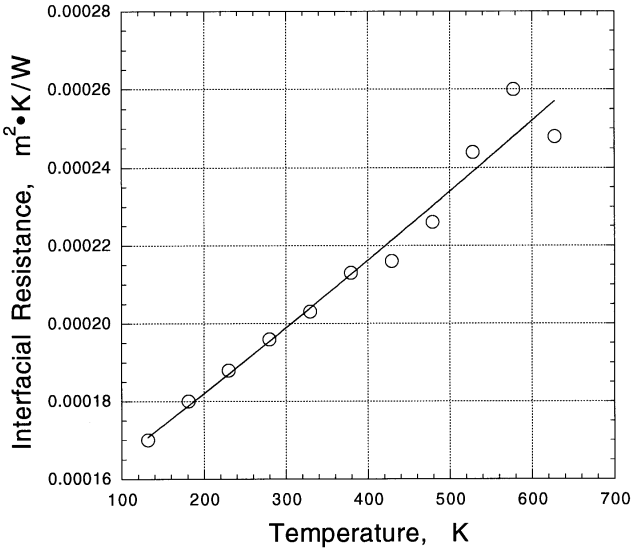

Fig. 4 Interfacial resistance between the measurement plates and 410 stainless steel

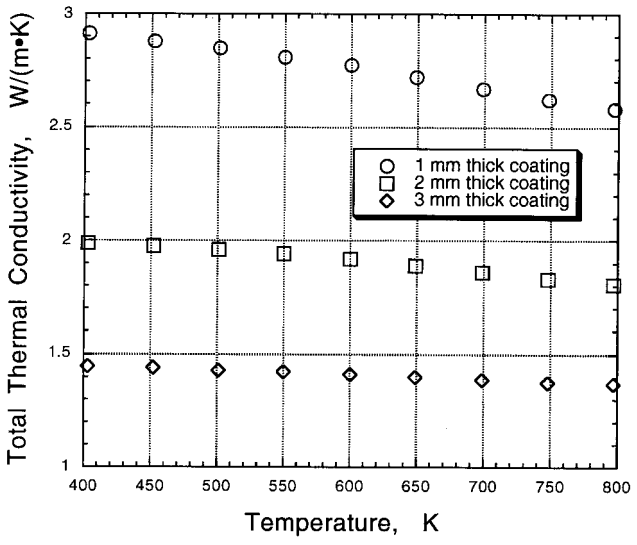

Fig. 5 Total thermal conductivity of the substrate coating system

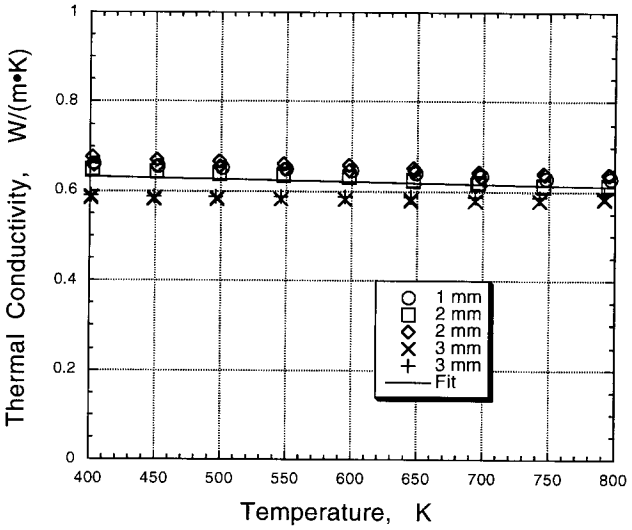

Fig. 6 Thermal conductivity of an atmospheric plasma-sprayed 8YSZ coating

tervals of 50 K back up to the maximum temperature. During the first temperature ramp, which is designated as the conditioning run, the specimen and plates mechanically settle, helium diffuses along the interfaces, and metallic specimens oxidize. A dwell time of at least three hours is maintained at each temperature point to establish steady-state thermal conditions.

This conditioning is imperative for the measurement since the interfacial resistances change during this time, but then settle into repeatable values. After the interfaces have stabilized, the second and all subsequent temperature ramps provide stable and repeatable measurements. Only these stable data are used to determine thermal conductivity and interfacial resistance.

Figure 5 plots the total conductivity of the substrate-coating system for the three coating thicknesses. The total conductivity is the reciprocal of four resistivity values: the thermal resistance of the coating, thermal resistance of the stainless steel substrate, interfacial resistance between the measurement plates and the substrate, and interfacial resistance between the measurement plates and the coating. Since the total conductivity represents the reciprocal of the sum of the resistivities of all of these values, it strongly depends on the thickness of the coating. As the thickness of the thermal barrier coating increases, as does the resistivity of the coating, the observed total conductivity decreases.

When data from the three 8YSZ coating thicknesses were analyzed, values for thermal conductivity of the coating fell within a narrow range centered around 0.62 W/(m·K). Figure 6 shows thermal conductivity for the 8YSZ coating. Data for all three coating thicknesses are shown. The line shows the mean of all of the data. The slight differences in the data could represent small variations in the coating microstructure. These data were reduced using a linear fit of interfacial resistance between the coating and thermocouple plate as a function of the surface finish of the coating. All of the data lie within 7% of the mean value, which is slightly outside of the estimated uncertainty of the measurement. Using a linear function for interfacial resistance may be an oversimplification which would result in additional systematic errors for this set of tests. Thermal conductivity appears to decrease slightly with increasing temperature, but for practical purposes may be considered independent of temperature over the range of temperatures tested here.

4. Conclusions

The authors measured thermal conductivity of an air plasma-sprayed 8YSZ coating using an absolute, steady-state technique from 400 to 800 K. An average thermal conductivity value of 0.62 W/(m·K) was determined for the 8YSZ coating over this range of temperature. Only a slight temperature dependence was observed over the temperature range tested. In the course of this analysis, the thermal conductivity of 410 stainless steel was also measured using the same steady-state technique. The thermal conductivity of 410 stainless steel at 400 K was 20.5 W/(m·K).

Acknowledgment

This work was partially supported under NSF-MRSEC-DMR9632570.

References

1. M.F. Gruninger and M.V. Boris, Thermal Barrier Ceramics for Gas Turbine and Reciprocating Heat Engine Applications, *Thermal Spray: International Advances in Coatings Technology*, C.C. Berndt, Ed., ASM International, 1992, p 487-492
2. S. Bose and J. DeMasi-Marcin, Thermal Barrier Coating Experience in Gas Turbine Engine at Pratt & Whitney, *Thermal Barrier Coating Workshop*, NASA CP-3312, 1995, p 63-73
3. F.O. Soechting, A Design Perspective on Thermal Barrier Coatings, *Thermal Barrier Coating Workshop*, NASA CP-3312, 1995, p 1-15
4. C.C. Berndt, R. Ratnaraj, J. Karthikeyan, and Y.D. Jun, Material Property Variations in Thermally Sprayed Coatings, *Thermal Spray Coatings: Properties, Processes and Applications*, T.F. Bernecki, Ed., ASM International, 1992, p 199-204
5. "Standard Test Method for Steady State Heat Flux Measurements and Thermal Transmission Properties by Means of the Guarded-Hot-Plate Apparatus," C 177-85, *Annual Book of ASTM Standards*, Vol 6, ASTM, 1988, p 17-28
6. B.J. Filla, Design and Fabrication of a Miniature High-Temperature Guarded-Hot-Plate Apparatus, *Thermal Conductivity,*, Vol 21, Plenum Press, New York, 1990, p 67-74
7. B.J. Filla, A Steady-State High-Temperature Apparatus for Measuring Thermal Conductivity of Ceramics, *Rev. Sci. Instrum.*, 68:7, July 1997, p 2822-2829
8. W.H. McAdams, *Heat Transmission*, 2nd ed., McGraw-Hill, 1942, p 7
9. W.J. Brindley, Properties of Plasma Sprayed Bond Coats, *Thermal Barrier Coating Workshop*, NASA CP-3312, 1995, p 189-202
10. R. Brandt, L. Pawlowski, G. Neuer, and P. Fauchais, Specific Heat and Thermal Conductivity of Plasma Sprayed Yttria-Stabilized Zirconia and NiAl, NiCrAl, NiCrAlY, NiCoCrAlY Coatings, *High Temp.-High Press.*, Vol 18, 1986, p 65-77
11. F.G. Sherif, L.J. Shyu, J.E. Jonkouski, and T.F. Bernecki, Evaluation of Sol-Gel 8% Yttria Stabilized Zirconia Powder for Gas Turbine Thermal Barrier Coatings, *Thermal Spray: International Advances in Coatings Technology*, C.C. Berndt, Ed., ASM International, 1992, p 505-511
12. Y.S. Touloukian, R.W. Powell, C.Y. Ho, and P.G. Klemens, *Thermophysical Properties of Matter, TPRC Data Series*, Vol 1, Plenum Press, New York, 1970, p 1148-1151